Nuclear Instruments and Methods in Physics Research B xxx (2016) xxx–xxx

Contents lists available at ScienceDirect

Nuclear Instruments and Methods in Physics Research B

journal homepage: www.elsevier.com/locate/nimb

Fröhlich resonance in carbon nanospiroids and the 2175 Å interstellar absorption feature

Sergey Yastrebov [a,*], Maxim Chekulaev [a], Alexandra Siklitskaya [b], Jacek A. Majewski [b], Roger Smith [c]

[a] A.F. Ioffe Physicotechnical Institute, St. Petersburg, Russia
[b] Theoretical Physics Institute, Warsaw, Poland
[c] School of Science, Loughborough University, Loughborough LE11 3TU, United Kingdom

ARTICLE INFO

Article history:
Received 31 July 2016
Received in revised form 15 August 2016
Accepted 6 September 2016
Available online xxxx

Keywords:
Collisions
Nanoclusters
Carbon
Diamond
Graphene
Novel forms of carbon

ABSTRACT

This paper demonstrates that a free electron gas model accurately simulates the spectral dependence of optical extinction spectra for carbon spiroids under the assumption that free electrons are confined in an homogeneous spherical particle owing to the delocalisation of π electrons that occurs in the actual spectral range. This effect can occur in the spiroid, rather than a spheroid (onion) due to the variable radii of the spiral turns as a function of distance from the centre, which are smaller than typical values for the spheroid.

1. Introduction

Analysis of the optical emission spectra from the stellar structure HD97048 indicates the presence of small diamonds in the interstellar medium due to the emission bands at 3.43–3.53 mkm [1]. These bands are fingerprints of nanodiamonds and occur together with the emission band at 3.3 mkm that is the fingerprint of graphene [1,2]. The size of the nanodiamonds is known from the analysis of meteors and lies in the region of 1.2–1.4 nm in diameter [3]. Nanodiamonds possibly form in carbon stars and are emitted into the interstellar region by the star wind. The most favourable mechanism of their formation is through a collision process of carbon ions. During ejection from the carbon star and subsequent travel through the universe, diamond nanoclusters undergo irradiation which causes their heating to a temperature whereby a transition from nanodiamond to carbon nanospiroid occurs as was shown in [3].

The transition to a spiroid form under irradiation is more likely than transition to a spheroid because these structures are less symmetric and can form from defective nanodiamonds more easily through radiation induced defects and skeleton strain [3–5].

Such structures that have been formed from nanodiamonds by irradiation have well defined optical properties which can act as their fingerprints. It is the optical properties of these irradiated structures that are the focus of this paper. We establish a correlation between optical properties of carbon nano-spiroids and the 217.5 nm interstellar optical extinction band. Details of this band are presented elsewhere, see, e.g., [6–8]). Carbon nano-spiroids have smaller distances between the turns than the inter-shell spacings for the spheroid (onion) and the spiroid can be filled up with electrons homogeneously owing to field-induced interturn tunneling. Consequently, we use here the first (dipole) term of Mie series for decomposition of the extinction cross section for homogeneous sphere presented in [9] and termed there as electrostatic approximation.

2. The model

Here we perform Density Functional Theory (DFT) calculations using Car–Parrinello Molecular Dynamics (CPMD) for geometry optimisation of the $C_{60}@C_{240}$ carbon spheroid and the C_{300} carbon spiroid to derive the interatomic distances between successive layers for estimation of the optical properties.

In order to do this we used approximate coordinates from Osawa's spiroid [10]. combined with an algorithm that produces the C_{60} and C_{240} double-shell spheroid and the C_{300} spiroid from [11].

* Corresponding author.
E-mail address: Yastrebov@mail.ioffe.ru (S. Yastrebov).

http://dx.doi.org/10.1016/j.nimb.2016.09.008
0168-583X/

The resulting $C_{60}@C_{240}$ multiwall fullerene (spheroid) and C_{300} spiroid are shown in Fig. 1(a) and (b), respectively. The mathematical model of such a spiroid has been described in our earlier articles and the graphical image of it is presented in Fig. 1(c).

As one can see, the spiroid and spheroid (carbon onion) exhibit differences in their geometries. The characteristic feature of the spiroid is the opening hole with a passage that constitutes a quasi two-dimensional channel that ends up in the spiroid's centre of mass. Measurements have shown that the width of the entrance hole is around 9.3 Å, while the spacing between the adjacent shells within the channel varies from 2.8 Åat the edge to 3.6 Åin the middle of the channel. Geometries of the spheroid and spiroid were optimised first using the Avogadro molecular editor with the UFF model [12] before they were input to CPMD [13] with the Nose thermostat [14], where the final optimisation of geometry was performed for zero temperature. A plane wave basis set with a cutoff of 50 Ry and the PBE exchange–correlation potential was used for the calculations. The long-range van der Waals interaction was accounted for by means of a semi-empirical DFT-D2 approach proposed by Grimme [15]. The shapes of the spiroid and spheroid after the resulting optimisation of the geometry are identical to the eye as those shown in Fig. 1a and b. Analysis shows that while increments, i.e. intershell distances for the case of carbon nanospheroid equal approximately to 3.4 Å, the distances between the successive turns of spiroid (increments) for the case of spiroid presented in Fig. 1 are smaller and are shown in Fig. 2. Therefore, the tunnel probability for electrons is bigger for the case of spiroid. Actually, DFT *abinitio* studies by [16] have also shown that an electric field perpendicular to a graphene plane does not noticeably introduce additional electrons into the conduction band of the graphene plane, in the spectral region ($0 - \sim 10$ eV). For the component parallel to the graphene plane ("in plane" or tangential component), π electrons solely contribute to the optical properties in the $\hbar\omega \approx 4.5$—$\hbar\omega \approx 7$ eV spectral region [16]. By analogy with graphite the potential barrier for electrons is about the value of work function ≈4.6 eV [17]. Thus, for photon energies exceeding the barrier height, both carbon multishell spiroids and spheroids fill up with electron gas. Bearing in mind tunnel mechanism of electron motion, it seems quite natural to use the model of a sphere filled up with free electron gas of π electrons for estimation of optical properties of carbon nanospheroids and nanospiroids, though probability of interturn tunnelling is bigger for spiroids.

2.1. The formalism of optical absorption

A model for the optical properties is now presented. We shall start from the dielectric function ϵ of free electron gas [9]:

$$\epsilon_1 = \epsilon_\infty - \frac{\omega_\pi^2}{\omega^2 + \gamma^2} \tag{1}$$

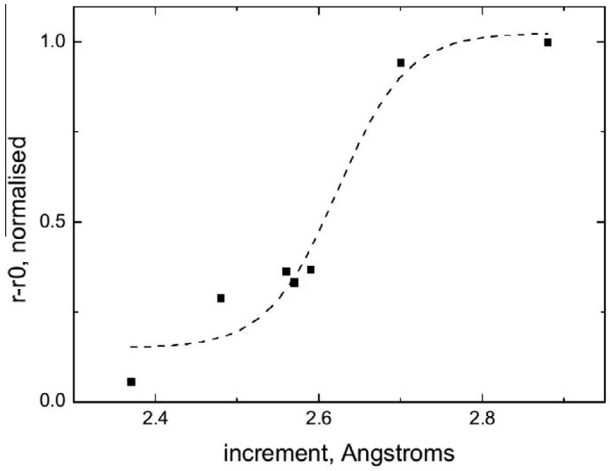

Fig. 2. The interatomic distances between adjacent spirals in the spiroid shown in Fig.1. Black squares stand for measurements and the dashed line shows trend.

$$\epsilon_2 = \frac{\omega_\pi^2 \gamma}{\omega(\omega^2 + \gamma^2)} \tag{2}$$

$$\epsilon_\infty = \frac{\omega_\pi^2}{\omega_\pi^2 + \gamma^2} \tag{3}$$

$$\epsilon = \epsilon_1 - i\epsilon_2 \tag{4}$$

here $\gamma = \frac{1}{\tau}$ is the inverse relaxation time ϵ_1 and ϵ_2 are the real and imaginary parts of the dielectric function, ω is frequency of photon, and the complex dielectric function of free electron gas is ϵ.

The polarisability of a vacuum-suspended spherical particle containing damped electron gas α with radius R obeys the equation [9]:

$$\alpha = R^3 \frac{\epsilon - 1}{\epsilon + 2} \tag{5}$$

Substituting ϵ with real and imaginary parts defined by (1–4) into Eq. (5), gives:

$$Re(i\alpha) = R^3 \frac{3\epsilon_2}{\epsilon_2^2 + (2 + \epsilon_1)^2} \tag{6}$$

Optical extinction of an ensemble of spherical particles in the Rayleigh-Gans model is determined through the extinction cross-section calculated for the single particle multiplied by the number of scatterers per unit volume [9]. It is known that the optical extinction cross section Q_r induced by an ensemble of M equiva-

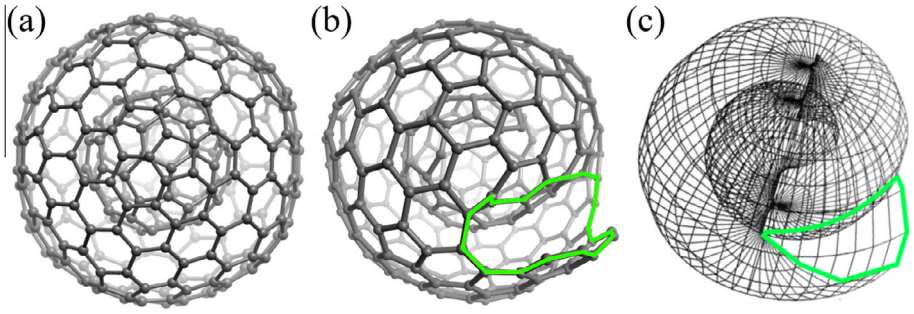

Fig. 1. (a) Example of the multishell fullerene C_{300}-carbon onion; (b) Typical spiroid obtained as a combination of C_{60} and C_{240} fullerenes (as described in the text); (c) Geometrical model of the spiroid (see the detailed description in the text). The spheres indicate atoms and sticks chemical bonds between carbon atoms. The green colour indicates the edge of the spiroid's entrance. (For interpretation of the references to color in this figure legend, the reader is referred to the web version of this article.)

Please cite this article in press as: S. Yastrebov et al., Fröhlich resonance in carbon nanospiroids and the 2175 Å interstellar absorption feature, Nucl. Instr. Meth. B (2016), http://dx.doi.org/10.1016/j.nimb.2016.09.008

lent vacuum-suspended single particles having a size much smaller than the wavelength of the radiation obeys the following expression:

$$Q = M4\pi kRe(i\alpha) \tag{7}$$

where $k = \frac{2\pi}{\lambda}$ is wavenumber for a wave of wavelength λ; α is the polarisability of an extincting globular particle suspended in vacuo. Taking into account Eqs. (6) and (7), gives:

$$Q = 12\pi\frac{\omega}{c}R^3\frac{\epsilon_2}{\epsilon_2^2 + (2+\epsilon_\infty)^2} \tag{8}$$

We omitted here the number of particles M because of the normalised units available for experimental and interstellar extinction profiles. For correction of the monotonic trend in the interstellar extinction associated with extinction by silicate grains, we use the polynomial

$$Q' = \delta_0 + \delta_1\omega + \delta_2\omega^2 + \delta_3\omega^3 \tag{9}$$

addition to Eq. (8). This form is termed by us as "the baseline". And the resulting extinctrion $Q_r = Q + Q'$.

2.2. The numerical fitting

For simultaneous estimation of the relaxation time and the plasma frequency, Eq. (8) was fitted to the literature experiment data that are portrayed with solid grey circles in Fig. 3. The result of the fit is presented in Figs. 3 and 4 by the solid line with parameters given in the figure caption. A good agreement is seen in Fig. 3 between the fit and digitised data over most of the spectral region. The mean literature interstellar extinction curve is represented by the open circles in Fig. 4. For estimation of the model parameters Eq. (8) with added baseline polynomial (9) was fitted to the literature data. The results of the fit are shown by the solid full lines and fitting parameters values are presented in the figure captions. One may see that for both cases the π plasmon energy obtained in the course of fitting attains a value typical for graphite (see, e.g. [16]).

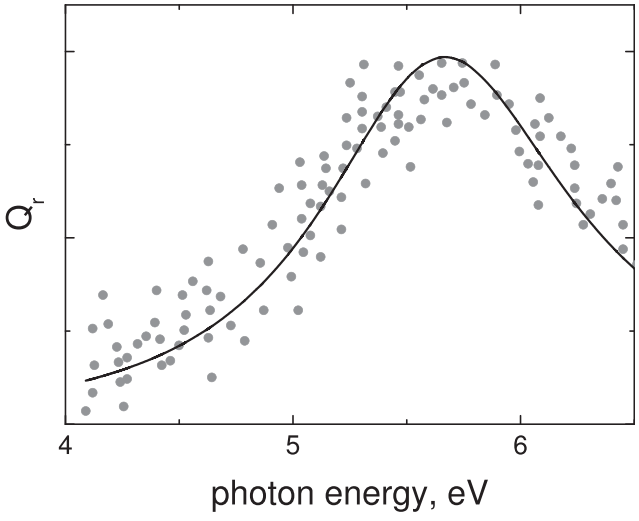

Fig. 3. The optical extinction cross-section for carbon onions as a function of photon energy. The grey circles are the experiment results for carbon onions given in [8]. The full line corresponds to the best fit by Eq. (8) to the experimental data (with outliers omitted) for the following set of parameters: $\epsilon_\infty = 1.432$, $\hbar\omega_\pi = 10.405 \pm 0.03$ eV, $\frac{\tau}{\hbar} = 0.562 \pm 0.02\ eV^{-1}$, $Q' = 0$.

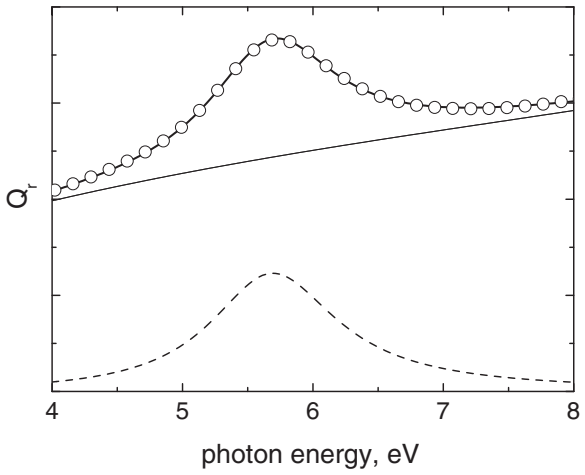

Fig. 4. Part of the mean interstellar extinction profile [7,8], represented by circles. The solid full line corresponds to the best fit of Eq. (8) to the data for the following set of parameters: $\epsilon_\infty = 1.432$, $\hbar\omega_\pi = 10.43 \pm 0.001$ eV, $\frac{\tau}{\hbar} = 0.797 \pm 0.001$, eV^{-1}. The thin line portrays the polynomial baseline. The dashed line shows the residual between the original profile and the restored baseline with parameters: $\delta_0 = 0$, $\delta_1 = 0.874$, $\delta_2 = -0.084$, $\delta_3 = 0.00377$ in normalised units.

3. Conclusions

Results of optimisation of the geometry of Osawa's spiroid shows a variation in the value of the radius vector with the distance from the spiroid's centre, with the inter-turn distances smaller than the inter-shell spacings for a carbon spheroid (onion). This provides evidence for the presence of an electron gas filling up the volume of a spiroid more effectively than a spheroid. The model of Fröhlich resonance with a π plasmon energy typical for graphite fits reasonably well the experimental absorption spectrum together with the mean interstellar extinction curve, in the area where the optical absorption 2175 Åband becomes dominant.

Acknowledgements

We would like to thank all COSIRES participants who indicated interest in our results and to Malcolm Heggie for fruitful discussion.

References

[1] O. Guillois, G. Ledoux, C. Reynaud, Diamond infrared emission bands in circumstellar media, Astrophys. J. 521 (1999) L133–L136, http://dx.doi.org/10.1086/312199.
[2] D. Grill, V. Pate, Characterization of diamondlike carbon by infrared spectroscopy?, Appl Phys. Lett. 60 (1992) 2089–2091, http://dx.doi.org/10.1063/1.107098.
[3] S.G. Yastrebov, R. Smith, A.V. Siklitskaya, Evolution of diamond nanoclusters in the interstellar medium, Mont. Not. R. Astron. Soc. 409 (2010) 1577–1584, http://dx.doi.org/0.1111/j.1365-2966.2010.17399.x.
[4] S. Yastrebov, A. Siklitskaya, R. Smith, Variable step radial ordering in carbon onions, Diamond Relat. Mater. 32 (2013) 32–35, http://dx.doi.org/10.1016/j.diamond.2012.11.012.
[5] S. Yastrebov, A. Siklitskaya, R. Smith, Structure-induced negatively skewed X-ray diffraction pattern of carbon onions, J. Appl. Phys. 114 (2013), http://dx.doi.org/10.1063/1.4824286, 134305-1–134305-4.
[6] S. Yastrebov, R. Smith, Nanodiamonds enveloped in glassy carbon shells and the origin of the 2175 optical extinction feature, Astrophys. J. 697 (2) (2009) 1822–1826, http://dx.doi.org/10.1088/0004-637X/697/2/1822.
[7] S.G. Yastrebov, R. Smith, The contribution of carbon nanoparticles to the interstellar optical extinction, Mon. Not. R. Astron. Soc. 395 (2009) 401–409, http://dx.doi.org/10.1111/j.1365-2966.2009.14527.x.
[8] M. Chhowalla, H. Wang, N. Sano, K.B.K. Teo, S.B. Lee, G.A.J. Amaratunga, Carbon onions: carriers of the 217.5 nm Interstellar Absorption Feature, Phys. Rev. Lett. 90 (2003), http://dx.doi.org/10.1103/PhysRevLett.90.155504, 155504-1–155504-4.
[9] C.F. Bohren, D.R. Huffman, Absorption and Scattering of Light By Small Particles, Wiley, New York, 1998.

[10] M. Ozawa, H. Goto, M. Kusunoki, E. Osawa, Continuously Growing Spiral Carbon Nanoparticles as the Intermediates in the Formation of Fullerenes and Nanoonions, J. Phys. Chem. B. 106 (2002) 7135–7138, http://dx.doi.org/10.1021/jp025639z, past 12.
[11] Cn fullerenes, URL http://www.nanotube.msu.edu/fullerene/fullerene-isomers.html, last visited 29.07.2016.
[12] M.D. Hanwell, D.E. Curtis, D.C. Lonie, T. Vandermeersch, E. Zurek, G.R. Hutchison, Avogadro: an advanced semantic chemical editor, visualization, and analysis platform, Cheminformatics 4 (2012) 1–17, http://dx.doi.org/10.1186/1758-2946-4-17.
[13] R. Car, M. Parrinello, Unified approach for molecular dynamics and density-functional theory, Phys. Rev. Lett. 55 (1985) 2471–2474, http://dx.doi.org/10.1103/PhysRevLett. 55.2471.
[14] S. Nose, A unified formulation of the constant temperature molecular dynamics methods, J. Chem. Phys. 81 (1984) 511–519, http://dx.doi.org/10.1063/1.447334.
[15] S.J. Grimme, Semiempirical GGA-type density functional constructed with a long-range dispersion correction, Comput. Chem. 27 (2006) 1787–1799, http://dx.doi.org/10.1002/jcc.20495.
[16] A.G. Marinopoulos, L. Reining, A. Rubio, V. Olevano, Ab initio study of the optical absorption and wave-vector-dependent dielectric response of graphite, Phys. Rev. B 69 (2004), http://dx.doi.org/10.1103/PhysRevB.69.245419, 245419-1245419-12.
[17] K.S. Krisenan, C. Jain, Thermionic Constants of Graphite, Nature 26 (1952) 702–703, http://dx.doi.org/0.1038/169702c0.

Please cite this article in press as: S. Yastrebov et al., Fröhlich resonance in carbon nanospiroids and the 2175 Å interstellar absorption feature, Nucl. Instr. Meth. B (2016), http://dx.doi.org/10.1016/j.nimb.2016.09.008